RSC Advances

PAPER

View Article Online
View Journal | View Issue

Cite this: *RSC Adv.*, 2023, **13**, 28993

Redox cationic frontal polymerization: a new strategy towards fast and efficient curing of defect-free fiber reinforced polymer composites†

Muhammad Salman Malik, Markus Wolfahrt and Sandra Schlögl *

Frontal polymerization of epoxy-based thermosets is a promising curing technique for the production of carbon fiber reinforced composites (CFRCs). It exploits the exothermicity of polymerization reactions to convert liquid monomers to a solid 3D network. A self-sustaining curing reaction is triggered by heat or UV-radiation, resulting in a localized thermal reaction zone that propagates through the resin formulation. To date, frontal polymerization is limited to CFRCs with a low fiber volume percent as heat losses compromise on the propagation of the heat front, which is crucial for this autocatalytic curing mechanism. In addition, the choice of suitable epoxy monomers and thermal radical initiators is limited, as highly reactive cycloaliphatic epoxies as well as peroxides decarboxylate during radical induced cationic frontal polymerization. The resulting networks suffer from high defect rates and inferior mechanical properties. Herein, we overcome these shortcomings by introducing redox cationic frontal polymerization (RCFP) as a new frontal curing concept. In the first part of this study, the influence of stannous octoate (reducing agent) was studied on a frontally cured bisphenol A diglycidyl ether resin and mechanical and thermal properties were compared to a conventional anhydride cured counterpart. In a subsequent step, a quasi-isotropic CFRC with a fiber volume of >50 vol%, was successfully cured *via* RCFP. The composite exhibited a glass transition temperature > 100 °C and a low number of defects. Finally, it was demonstrated that the redox agent effectively prevents decarboxylation during frontal polymerization of a cycloaliphatic epoxy, demonstrating the versatility of RCFP in future applications.

Received 1st September 2023
Accepted 25th September 2023

DOI: 10.1039/d3ra05976f

rsc.li/rsc-advances

1. Introduction

Radical induced cationic frontal polymerization (RICFP) has gained a lot of attention amongst researchers in the past few years, as a rapid curing substitute for various cyclic ether monomers.[1–7] The well-known cationic frontal polymerization involves generation of radicals and cations when diaryliodonium salts are photo or thermal cleaved, when subjected to ultraviolet light or heat. A strong Brønsted acid is produced that protonates cyclic ether monomers forming highly reactive cations that are able to react with adjacent cyclic ether groups forming polyether in a ring opening cationic polymerization. The heat of polymerization is then utilized to homolytically cleave a thermal radical initiator and a hot front propagates by the thermally generated radicals, which are oxidized to cations in the presence of an iodonium salt. Unreacted monomers are consumed in the absence of UV light deep within the bulk of the monomer resin.[8] Up till now, frontal polymerization has been successfully demonstrated in the UV-induced curing of epoxy-based carbon fiber reinforced composites however, limited to a certain thickness of the composite and fiber volume percent.[3,4,9] This limitation comes from the fact that carbon fibers are intrinsically UV blockers leading to a top cured surface and an uncured resin in through thickness direction of the composite. This means that for structural components in automotive and aerospace industries, where the thickness of carbon fiber reinforcements could easily reach up to 50 mm, an incomplete curing of the composite would lead to catastrophic operational failure and loss of mechanical properties. On the contrary, currently reported fiber volume of <50 vol% by various authors are not suitable for industrial application, where high composite thicknesses are necessary.[3,4,9]

Alternatively, the front has to be initiated by a very high temperature source such as infra-red, or the entire epoxy impregnated composite has to be exposed to at least 250 °C in an oven.[10] However, at these high temperatures the initiators and monomers might already evaporate and the formed epoxy network starts to degrade.[11] Typically, with peroxide initiators, release of CO_2 and other volatile organics are unavoidable when exposed to high temperatures and this results in disintegration of the formed network's properties due to the formation of

Polymer Competence Center Leoben, Rossegerstraße 12, 8700 Leoben, Austria. E-mail: sandra.schloegl@pccl.at

† Electronic supplementary information (ESI) available. See DOI: https://doi.org/10.1039/d3ra05976f

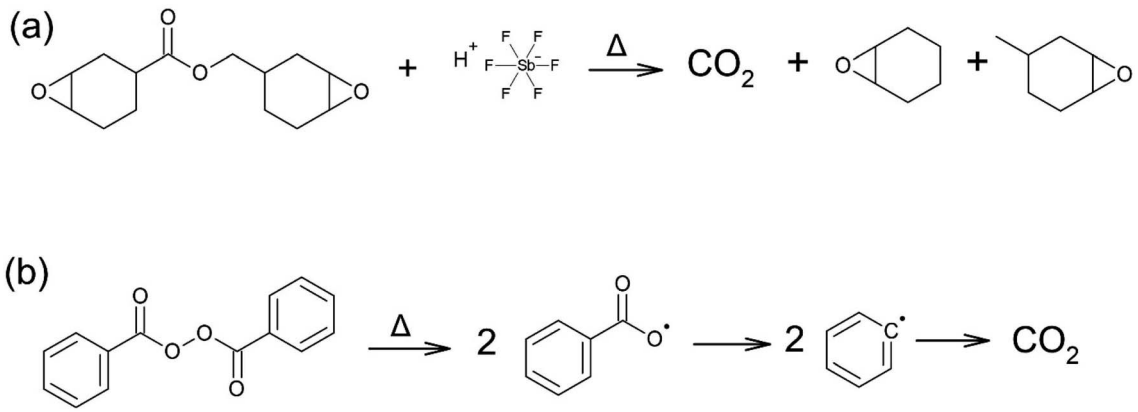

Scheme 1 (a) Reaction between a Brønsted acid and cycloaliphatic epoxy during RICFP and, (b) decarboxylation of cycloaliphatic epoxy yielding carbon centred radicals and carbon dioxide at elevated temperatures.

defects.[5,12] A more convenient way is to initiate the self-sustaining front at much lower temperatures (*e.g.* 100–130 °C), that is just sufficiently high to cleave the thermal radical initiator. This route of the reaction sequence would involve direct protonation of the cyclic ether monomer from the reaction between radical species and iodonium salt, thereby skipping the generation of a Brønsted acid. However, the growing oligomeric polyether chain achieves a low cross-linking density since the iodonium salt is not fully reduced to cations and radicals as in UV induced reaction during frontal curing. To ensure maximum cross-linking of the polymerizing cyclic ether under low oven temperatures during frontal curing, our studies found a unique approach, *i.e.*, to couple iodonium salt with a reducing agent to have a redox cationic frontal polymerization (RCFP).

Redox polymerizations were previously known in cationic (RCP) and mainly in free radical polymerizations (RFRP) that allows curing under mild conditions with reduced energy consumption.[13,14] The accelerating effect of reducing agents in thermal radical initiating systems were first reported back in 1937.[15–17] Remarkable works done by Garra *et al.* showed the possibility of combining various reducing agents with diaryliodonium salts for RFRP, RCP or combination of both. These dual curing process allowed formation of interpenetrating polymer networks and various composites.[13,18–22] In the field of frontal polymerization, redox frontal polymerization has been investigated only on free radically polymerizing monomers such as acrylates[23–26] and vinyl monomer,[27] where the emphasis was placed on decreasing front temperatures and to produce a defect-free cured polymer. For cyclic ether monomers following a RCP route, studies have shown that various reducing agents such as ascorbic acid,[28,29] benzoin,[30] tin(II) ethyl hexanoate (stannous octoate)[31] silanes,[32,33] dialkylborane[34] are able to form a highly efficient redox couple with diaryliodonium salts. Amongst these reducing agents, Crivello showed that the redox couple between stannous octoate and iodonium salt is highly efficient in curing various epoxy monomers with continuous medium temperature heat to a tack free polymer within few minutes.[35] If this redox couple is combined with a radical thermal initiator, it would ensure full exploitation of the diaryliodonium salt in the absence of UV light, while curing epoxy autocatalytically in through thickness of a fiber reinforced composite *via* a process now termed as RCFP.

Another challenge in RICFP is the instability of thermal radical initiators, especially those which are prone to volatilization such as peroxides.[5] For highly reactive cyclic ether monomers such as cycloaliphatic monomers, decarboxylation of monomer (Scheme 1a) and initiator volatilization (Scheme 1b) limits their usage in frontal polymerization.[36,37] Even though, recent works by Staal *et al.* showed that the physical characteristics of the mould governs the successful propagation of the hot front.[1] However, we observed in our experiments that even pinacol-based thermal initiator cannot prevent foaming in cycloaliphatic epoxies when higher initiator concentrations are needed to speed up the front.

In the current study, we report the applicability of stannous octoate as a reducing agent to address two major improvements in the cationic frontal polymerization of epoxy monomers; (i) increased conversion and mechanical properties of oven cured epoxy monomers commonly used in fiber reinforced composites, (ii) prevention of decarboxylation in cycloaliphatic epoxy when benzoyl peroxide (BPO) is used as thermal radical initiator. BPO and *N*,*N*-dimethylaniline redox couple has previously been shown to prevent bubbles in free radical frontal polymerization.[24,38] However, due to inherent toxicity of *N*,*N*-dimethylaniline, we did not proceed further in our experiments with this reducing agent. Stannous octoate has been chosen over other reducing agents in our studies due to its good miscibility in various epoxy monomers and also, it allows reduction in the amount of co-initiators as reported elsewhere.[39,40] Yilmaz *et al.* reported RCP formulation involving BPO, sulfonium salt and ascorbic acid reducing agent for ambient temperature curing of cyclic ether monomer.[41] However, this copper catalysed route to curing does not fall in the category of frontal polymerization. For the first time, we introduce the idea of a redox cationic frontal polymerization (RCFP) for rapid and effective curing of epoxy monomers and demonstrate its applicability in curing technically relevant epoxy-based resins.

2. Materials and method

2.1 Materials

Litestone 2130E (mixture of bisphenol A diglycidylether and 1,4-butanediol diglycidylether) and Litestone 2131H (tetrahydromethylphthalic anhydride) were supplied by Olin. *p*-Octyloxy phenyl phenyliodonium hexafluoroantimonate was obtained from Gelest and all other components from Sigma-Aldrich. All chemicals were used as received without further purification. Monomers and initiators used in the current work are shown in Fig. 1.

2.2 Preparation and curing of neat resins

For the preparation of the standard thermally curable formulation (Litestone-Ref), an equivalent amount of Litestone 2130E and Litestone 2131H were mixed with a speed mixer VM-200 (State Mix) for 5 min until a homogeneous resin formulation was obtained. Curing was performed in an oven at 90 °C for 1 h and then further 4 h at 110 °C in accordance to the technical data sheet of the supplier.

In addition, various types of frontally curable epoxy compositions were prepared. For Litestone-RICFP, 1.5 wt% of *p*-octyloxy phenyl phenyliodonium hexafluoroantimonate (Iod) as cationic photoinitiator and 1.5 wt% of benzopinacol (BP) as thermal radical initiator were added to Litestone 2130E for a bubble free intact polymer. Whereas, Litestone-RCFP was prepared, which contained 1.93 wt% of Iod, 0.48 wt% of benzopinacol and 0.97 wt% of stannous octoate (SO). The radical thermal initiator was ground with a pestle to a fine size before adding it to the formulation, which mas mixed with a speed mixer for 5 min at room temperature. The resin compositions were poured in an in-house prepared silicon or Teflon mould and subsequently cured in an oven at 150 °C for not more than 10 min to achieve a bubble-free self-sustaining hot front.

For decarboxylation experiments, Litestone 2130E was exchanged with epoxy cyclohexyl methyl 3,4-epoxy cyclohexane carboxylate containing 0.49 wt% of *p*-octyloxy phenyl phenyliodonium hexafluoroantimonate and 0.40 wt% of Luperox A75 (dibenzoyl peroxide) as thermal radical initiator. To evaluate the effect of stannous octoate on frontal curing, another composition was prepared additionally containing 0.42 wt% of stannous octoate. The components were weighted in a polypropylene cup and subjected to speed mixing for 5 min at room temperature. Samples were poured in aluminium cups and then irradiated for 5 s with UV light (306 mW cm^{-2}) using an Omnicure S1500 200 W lamp from Lumen Dynamics (maximum irradiance = 10 W cm^{-2}) with a 5 mm in diameter light guide, to initiate the curing front.

2.3 Preparation and curing of fiber reinforced composites

For the preparation of reinforced composites, a carbon fiber biaxial non-crimp fabric (NCF) ± 45° 300 gsm and 0°/90° (twill weave) 400 gsm, supplied by R&G Faserverbundwerkstoffe GmbH was used for preparing a 20 mm thick composite *via* vacuum infusion (Fig. 2). Only the Litestone-RCFP resin was infused within a vacuum bagged composite stack at −0.95 bar vacuum for at least an hour. Once the resin infusion was complete, the bag setup was closed tightly with metal clips and disconnected from the vacuum pump. Later, the entire composite in vacuum bag was placed in an oven at 150 °C for at least 30 min with two K-type thermocouples inserted at the bottom and middle of the stack. The cured composite was then cut into several small sections using an in-house water jet cutting machine to obtain samples for DSC measurements.

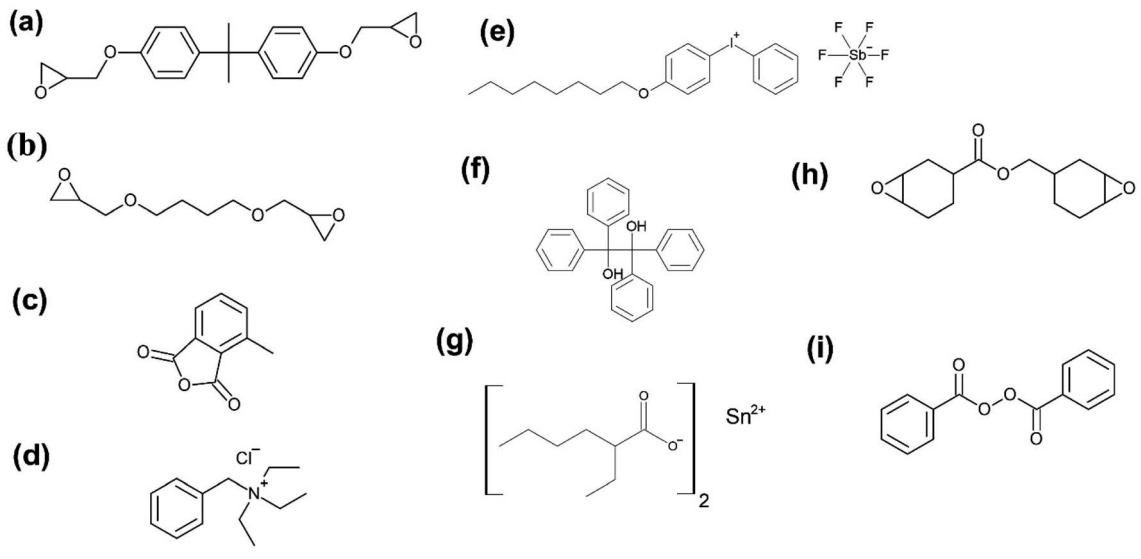

Fig. 1 Chemical structures of the various monomers and initiators used in the current study, (a) bisphenol A diglycidylether (Litestone 2130E) (b) 1,4-butanediol diglycidylether (Litestone 2130E), (c) tetrahydromethylphthalic anhydride (Litestone 2131H), (d) benzyl triethylammonium chloride (Litestone 2131H), (e) *p*-octyloxy phenyl phenyliodonium hexafluoroantimonate, (f) benzopinacol, (g) tin(II) ethyl hexanoate (stannous octoate), (h) 3,4 epoxy cyclohexyl methyl 3,4-epoxy cyclohexane carboxylate, (i) dibenzoyl peroxide.

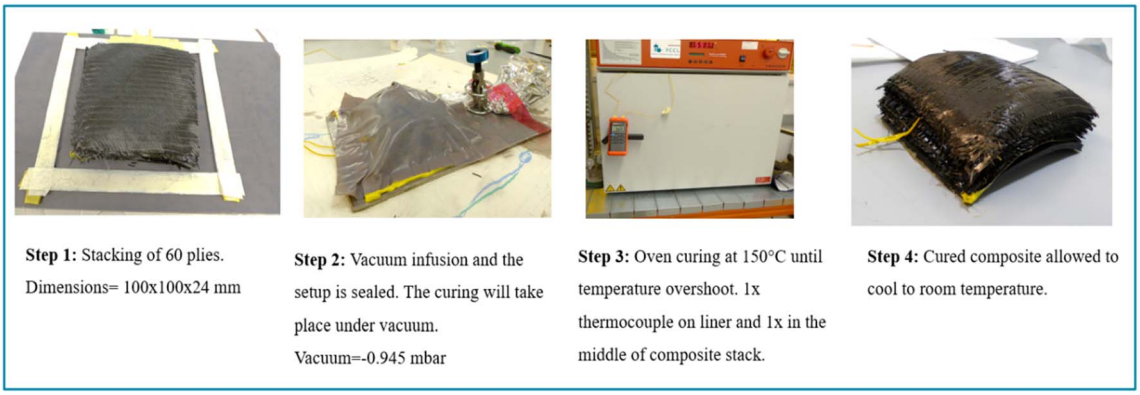

Fig. 2 Illustration and description of the stages involved in the preparation and curing of a CFRC cured *via* RCFP route.

2.4 Characterization

Fourier Transform Infrared (FT-IR) spectroscopy was done on cured samples using PerkinElmer Spectrum IR with attenuated total reflectance (ATR) accessory. The spectral range was between 600 and 4000 cm^{-1} with 16 scans per sample and resolution of 2 cm^{-1}. The degree of cure (α) was estimated by using eqn (1), in which $A_{915\ cm^{-1}}$ is the characteristic absorption band centered at 915 cm^{-1} for epoxy cyclic ethers and $A_{1509\ cm^{-1}}$ corresponds to the reference benzene ring absorption band at 1510 cm^{-1}, measured in cured and uncured state respectively.[42]

$$\alpha\ (\%) = 100\left(1 - \frac{A^{\text{cured}}_{\text{characteristic}}}{A^{\text{cured}}_{\text{reference}}} \Big/ \frac{A^{\text{uncured}}_{\text{characteristic}}}{A^{\text{uncured}}_{\text{reference}}}\right) \quad (1)$$

Non-isothermal DSC was performed using PerkinElmer 4000 on specimens (15–20 mg) cut from samples that were cured on the silicon or Teflon mould and aluminium cups for the two sets of experiments respectively. Two heating runs were performed on each sample with a heating rate of 20 °C min^{-1}. The first run was from 20 °C to 160 °C followed by cooling to 20 °C, and the second heating from 20 °C to 210 °C in agreement with DIN EN ISO 11357.[43] Each measurement was replicated twice and the mid-point glass transition temperature determined.

Viscosity of the resins was determined on an Anton Paar MCR 501 rheometer in frequency time-sweep mode. The plate–plate measurements were performed over a range of temperatures between 25 and 50 °C and with a shear rate equal to 100 s^{-1} for a time period of 100 s. Average from three measurements was taken.

Dynamic mechanical analysis (DMA) was performed on a Mettler Toledo DMA 861 in three-point bending mode according to DIN EN ISO 6721-5.[44] The specimens (70 × 10 × 3 mm) were cured in silicon moulds. DMA was performed for a temperature range from 0 to 220 °C at a heating rate of 2 °C min^{-1} with an oscillation of 1 Hz and 200% offset. The force and displacement were set to 40 N and 100 μm, respectively.

Tensile tests were performed on a Zwick Z250 machine with a pre-load of 0.25 MPa and a test speed of 2 mm min^{-1} according DIN EN ISO 5272.[45] The average of five measurements were taken.

3. Results and discussion

3.1 Frontal curing

In the first step, Litestone 2130E with varying amount of cationic photoinitiator (*p*-octyloxy phenyl phenyliodonium hexafluoroantimonate), thermal radical initiator (benzopinacol) and reducing agent (stannous octoate) were prepared to find a good balance between cure speed and optical quality of the obtained networks. The cured samples were visually inspected for defects, colour, cracking, *etc.*, and the formation of a propagating heat front was evaluated. Fig. 3 shows photographs of some examples of cured networks to detail how each component has an effect on the integrity and the quality of the specimen produced. If the amount of cationic photoinitiator exceeded 2 wt%, the sample was frontally curable but turned partly black and suffered from numerous defects (Fig. 3a). This behaviour can be explained by thermal degradation of the resin related to heat accumulation, similar to the results reported by Ma *et al.*[46] The same effect was obtained, albeit to a lower degree, when reducing the photoinitiator content to 2 wt% but keeping the benzopinacol concentration at 1 wt% (Fig. 3b). In contrast when the amount of stannous octoate was raised from 1 to 4 wt%, while keeping the photoinitiator and benzopinacol content constant at 2 and 1 wt%, respectively, the curing mechanism shifted more towards a purely cationic than frontal polymerization.[35] Thus, no front was observed and the resin required continuous heating to cure (Fig. 3c). The best performance (formation of a propagating curing front and defect-free specimen) was obtained by adding 2 wt% of the cationic photoinitiator, 1 wt% of stannous octoate and 0.5 wt% of the thermal radical initiator to Litestone 2130E. Once frontally cured, the network was defect-free with a light brown colour (Fig. 3d).

In the next step, the frontal temperatures were measured for the optimized resin formulation (Litestone-RCFP). In our studies, we did not encounter any differences in the front propagation or velocity when resins were oven cured in aluminium, Teflon or silicon moulds. Therefore, the effect of the thermal conductivity of the mould was considered as negligible in the current study since the resin and mould are

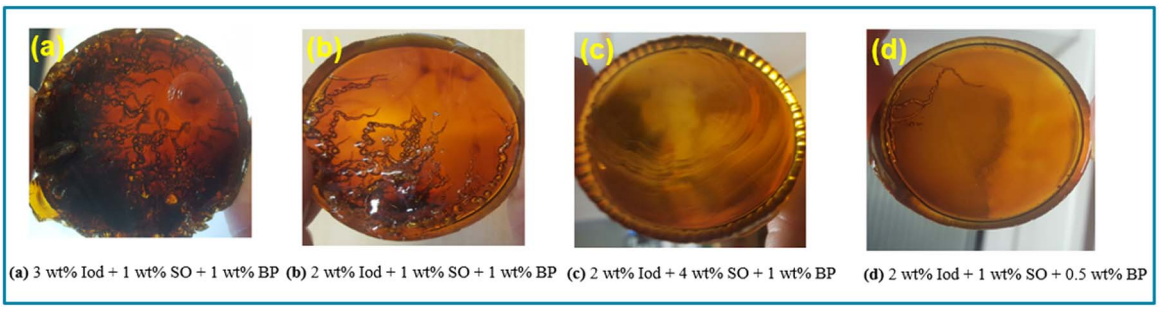

Fig. 3 Effect of initiator concentration on the structural integrity of the RCFP cured Litestone resin.

heated up continuously in the oven until a front is detected. Fig. 4a shows a 200 × 100 × 5 mm Teflon mould with two K-type thermocouples placed a distance apart. The Teflon mould was filled with Litestone-RCFP and kept in oven set to 150 °C for 10 min. The thermocouples were connected to a data logger and the graph (Fig. 4b) exhibits the minimum front onset and maximum front temperatures. The results show an onset at 130 °C with maximum front temperatures reaching up to 270 °C within 6 min confirming the formation of a propagating heat front typical for RICFP as reported in our previous study.[47]

The maximum exothermic temperatures on the two different points on the mold do not differ significantly as shown in Fig. 4b, and the cured resin was fully intact with no signs of degradation. The dark brown coloured spot in the middle of the cured plate is due to excessive heat accumulation, which arose during front initiation. If the resin was impregnated in a thermally conductive substrate or by adding thermally conductive fiber reinforcement (as will be shown in the following section), any heat accumulations could be safely prevented.

3.2 Thermal and mechanical properties of frontally cured neat resins

In order to characterize the changes in the degree of epoxy conversion between Litestone RCFP and RICFP cured resins, FT-IR ATR spectra were acquired and are shown in Fig. 5. However, it was not possible to evaluate changes in the cross-linking network based on these ATR results because there were no significant differences in epoxy conversion between RICFP and RCFP. Several samples were taken from various parts of the cured specimens and even then, the epoxy conversions remained significantly invariable, with Litestone-RICFP having 87% and 95% for Litestone-RCFP. This was probably due to the rapid vitrification of these frontally curable resins entrapping radicals and cations within the cross-linked network.[47] Therefore, DSC and DMA measurements were relied upon to verify from glass transition temperature measurements, if the cross-linking network was similar or different between Litestone-RICFP and RCFP cured resins.

Table 1 shows the comparison of the glass transition temperatures (T_g) of frontally cured Litestone resin (with and without stannous octoate) and a standard thermally anhydride cured counterpart as reference. The data of the anhydride cured resin is used as a benchmark for the frontally cured resins under investigation. The T_g values were obtained from DSC and DMA experiments. Additionally, Fig. 6 provides the storage modulus and tan delta curves of the three resins. In DSC, the midpoint T_g value of the reference network amounted to 90 °C, which is in good correlation to the onset storage modulus T_g

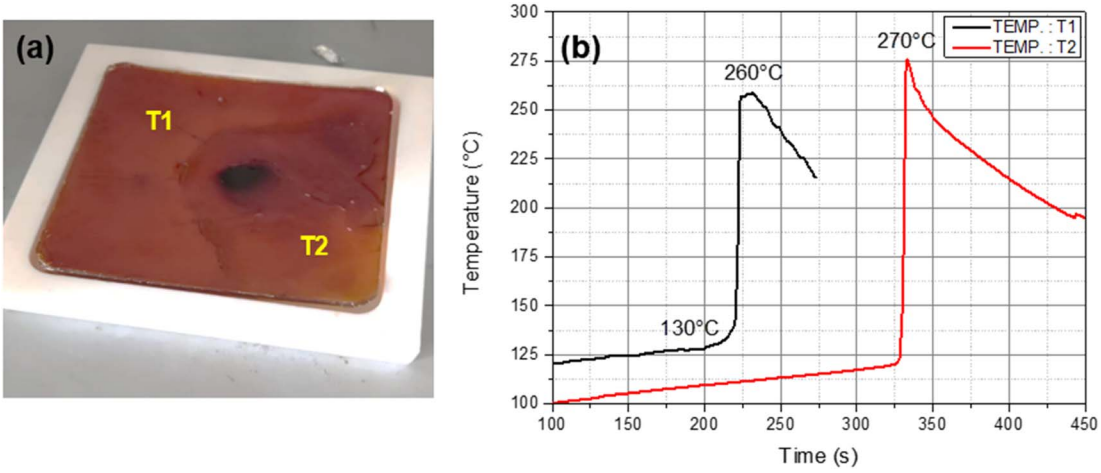

Fig. 4 (a) Frontal curing of Litestone-RCFP resin in a Teflon mold with position of thermocouple labelled (T1 and T2). (b) Temperature profile registered from the data logger of the two thermocouples after placing the mold in the oven at 150 °C.

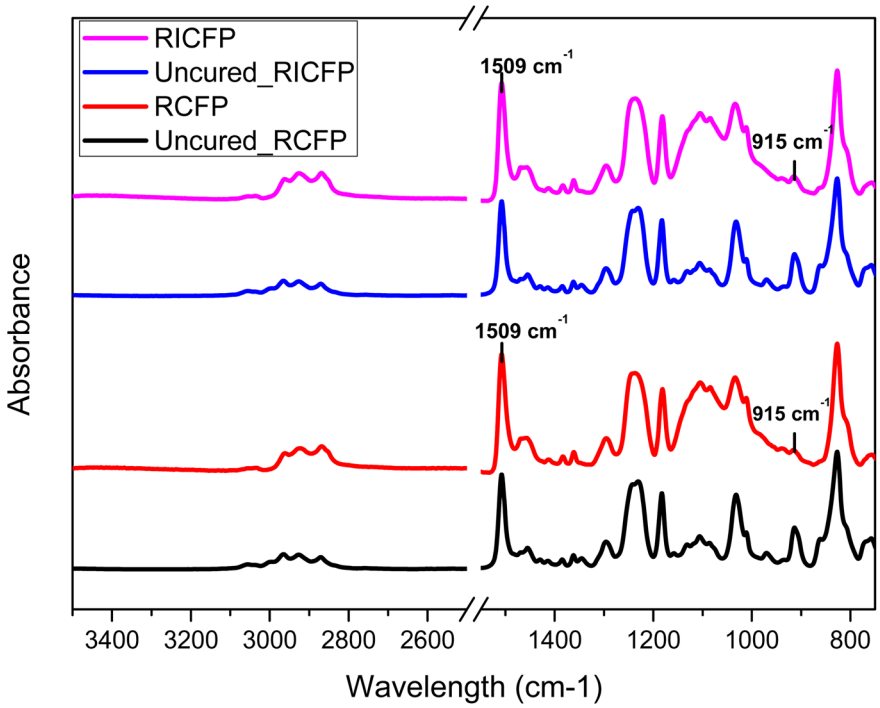

Fig. 5 FT-IR ATR spectra comparison between Litestone-RICFP and RCFP cured resins. The characteristic absorption band centered at 915 cm^{-1} was used for calculating epoxy conversion.

Table 1 Comparison of thermo-mechanical properties of the resins under investigation as obtained from DSC and DMA experiments

	DSC		DMA	
Formulation	First run mid-point T_g (°C)	Second run mid-point T_g (°C)	T_g onset E' (°C)	E' at 25 °C (GPa)
Litestone-Ref	90	107	87	3.9
Litestone-RCFP	90	112	88	4.9
Litestone-RICFP	50	78	45	3.2

obtained from DMA.[48] An increase in storage modulus above T_g is attributed to post curing effects according to the curing data available for anhydride cured Litestone resin. In the presence of stannous octoate, the frontally cured resin (Litestone-RCFP) was characterized by similar T_g values as the anhydride cured reference network (Table 1), while the storage modulus (E') was significantly higher. On the contrary, frontally cured Litestone-RICFP (without stannous octoate) had an onset T_g of around 50 °C, and underwent a distinctive post curing as shown by the shift of the midpoint T_g from 50 to 78 °C between the first and second DSC heating run.

The strong influence of stannous octoate on the T_g of the frontally cured epoxy resins is attributed to the differences in the cure kinetics which is expected to influence network structure. In an ideal radical induced frontal curing with benzopinacol, a strong Brønsted acid generated from photocleaved iodonium salt takes the lead in the generation of monomeric cations, followed by a curing front propagation due to carbon centred radicals produced as a result of thermal cleavage of benzopinacol.[8,36] Upon heating at 150 °C, the radical thermal initiator is cleaved first leading to the generation of carbon centred radicals in the early stages of cure. The iodonium salt photoinitiator is not cleaved at this moderate temperature and therefore reacts instantaneously with the carbon centred radicals to produce cations. This might have led to an earlier vitrification of the epoxy resin that entrapped radicals in the oligomeric structure preventing further access to epoxide groups. For this reason, a large difference between DSC midpoint T_g from the first and second heating runs for Litestone-RICFP is obtained as the second heating run recommenced polymerization and chain mobility allowing living cationic species to react further with epoxide groups. In the case of Litestone-RCFP, even though carbon centred radicals take the lead in front propagation, the highly efficient redox couple between iodonium salt and stannous octoate ensures generation of radicals and cations by lowering the charge of heteroatom of this iodonium salt.[31] This increases the number of radicals available for cationic ring opening and thus ensures a higher degree of cross-linking than conventional frontal route. Furthermore, a higher storage modulus at 23 °C is obtained for

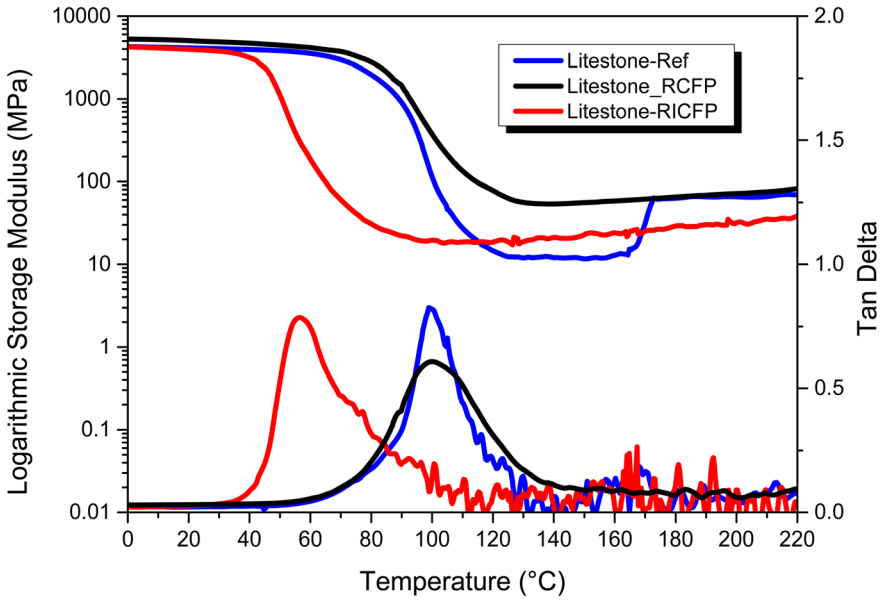

Fig. 6 Storage modulus and tan delta curves for the resins under investigation.

Litestone-RCFP (4.9 GPa) than the Litestone-RICFP having 3.2 GPa, also indicating a denser network with higher brittleness in the RCFP cured resin. To verify these results from DMA, the tensile moduli are shown Table 2 along with strength and elongation at break. A good correlation can be seen between DMA and tensile storage moduli for all three resins given in Tables 1 and 2.

To further verify the changes in T_g of the frontally cured Litestone resin with and without stannous octoate, cross-linking density of the two resins was evaluated from the DMA results.[49] In particular for Litestone-RICFP, the crosslink density amounted to 2200 mol m^{-3} whilst it was nearly doubled (5345 mol m^{-3}) for Litestone-RCFP. The results roughly show a two-fold increase in the cross-linking density with the addition of stannous octoate in the frontally cured Litestone resin. The higher glass transition temperature in Litestone-RCFP than Litestone-RICFP coincides well with this increase in cross-linking density. Therefore, stannous octoate shows a positive indication of its redox effect on the frontal curing of epoxy resin, by improving the thermomechanical properties.

The differences in network structure also govern mechanical properties of the thermosets as demonstrated by uniaxial tensile tests (Table 2). The frontally cured resins benefit from a higher tensile strength and elongation giving rise to a better toughness compared to the conventionally cured epoxy-anhydride system. However, Litestone-RCFP showed a better performance than Litestone-RICFP, which might be related to the difference in cure rate, network evolution and number of crosslink points.[47,50]

Table 2 Tensile properties of resins under investigation. Average values given along with standard deviation from 5 specimens for each formulation. Tensile curves for each formulation are provided in ESI

Formulation	Tensile strength (MPa)	Young's modulus (GPa)	Elongation at break (%)
Litestone-Ref	32 ± 2.7	3.4 ± 0.31	0.91 ± 0.11
Litestone-RICFP	45 ± 5.6	2.9 ± 0.40	1.90 ± 0.30
Litestone-RCFP	37 ± 5.6	3.4 ± 0.70	1.27 ± 0.30

3.3 Frontal curing of carbon fiber reinforced composites

Structural components based on fiber reinforced composites in aerospace or automobile industries are either quasi-isotropic and/or of very high thicknesses (>10 mm), where complete curing is often achieved after prolonged autoclave heating.[51] To demonstrate frontal curing of such components, a quasi-isotropic carbon fiber reinforced composite (CFRC) consisting of the following stack sequence was produced *via* vacuum infusion; $[(\pm 45°)_2/(0°/90°)_3]_2$; $[(\pm 45°)_2]$, using Litestone-RCFP with a fiber volume content of ~60 vol% (thermogravimetric graph given in ESI†). The viscosity of this resin ranged between 2500 and 300 mPa s (25–50 °C) and comprised a shelf life of more than 4 months.

A stack of 60 plies of CFRC was infused with Litestone-RCFP under vacuum and then heat cured in an oven at 150 °C until a thermal overshoot was detected. The graph for the curing time against temperature is shown in Fig. 7. The maximum front temperature reached 238 °C and the time to reach maximum front at the middle and bottom of the composite is only few seconds apart, indicating a good thermal distribution of the fibers over the composite thickness. A thermoplastic substrate placed at the bottom of the composite beneath the first thermocouple showed no signs of degradation during temperature overshoot (Fig. 7, inset). The composite was found to be tack free after 25 min of oven curing. Fig. 8 shows the optical micrograph taken from one cross-section of the cured CFRC. The optical image shows a good compaction and low number of voids. No signs of degradation of the resin or on the composite was seen.

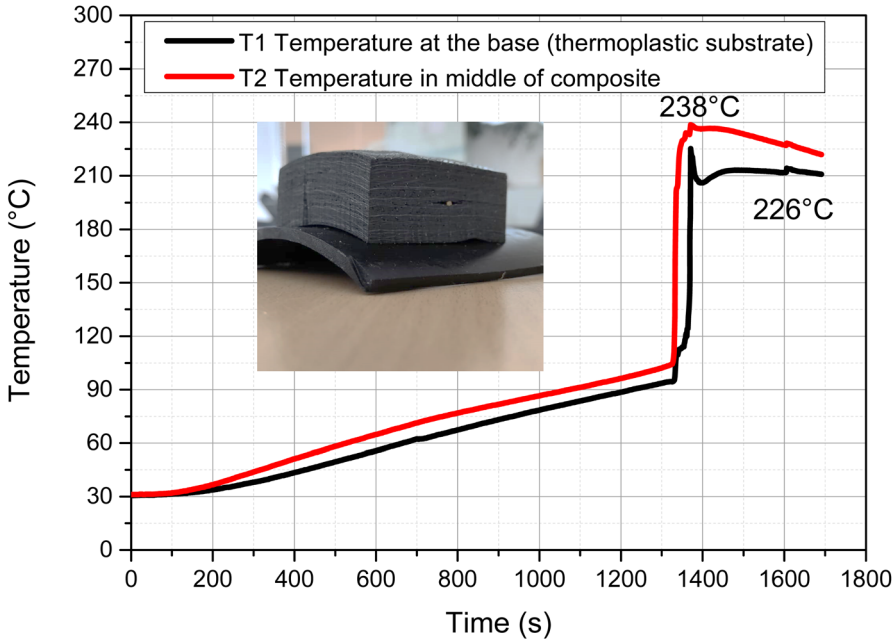

Fig. 7 Temperature profile of the frontally cured Litestone-RCFP in the CFRC composite. The two curves are registered from data logger with thermocouples placed in the corresponding positions labelled. Inset, picture of a 20 mm thick RCFP cured CFRC plate.

Fig. 8 Optical micrograph of the cross-section of the frontally cured CFRC plate obtained at a magnification of ×0.65 on a Zeiss optical microscope.

It was further of interest to know if the RCFP curing in the composite would indeed lead to a T_g similar to the neat resin. Therefore, samples for DSC measurement were cut from the thick composite into several sections. The midpoint T_g from first run gave a value of 115 °C from the first heating run followed by a midpoint value of 136 °C from the second heating run. Fillers or fibers have a positive impact on the propagation of frontally polymerizable resins, which might explain the distinctive increase in the T_g from neat resin to the composite.[2,52] The successful RCFP curing of high thickness CFRC showed that it is possible to cure such components under low oven heating and at a much shorter curing duration than conventional anhydride cured resins.

3.4 Prevention of decarboxylation in frontally cured cycloaliphatic epoxy resin

In further work, resin compositions consisting of cycloaliphatic epoxy were prepared, which have a higher reactivity than bisphenol A diglycidyl ether in frontal polymerization due to the higher exothermicity of the ring opening reaction.[53] However, at the same time they suffer from decarboxylation reactions, which compromise on the thermal and mechanical performance of the related networks. Herein, frontally curable resin formulations were prepared with (ECC-RCFP) and without (ECC-RICFP) stannous octoate using an organic peroxide as thermal initiator, which is also prone to decarboxylation at elevated temperature. ECC-RICFP was placed in an aluminium cup to visually follow the front propagation after activation by UV light. After 15 s irradiation, heavy fuming started followed by rapid bubble formation and degradation of the cured resin with a pungent odour (Fig. 9a). On the contrary, for ECC-RCFP, a stable and self-sustaining curing front free of any bubbles and negligible fumes was observed under the same UV irradiation conditions (Fig. 9b). The cured resin was completely intact and free of any entrapped bubbles.

The decarboxylation of the ester linkage in the backbone of the cycloaliphatic epoxy occurs as a result of thermal cleavage of the peroxy radical (Scheme 1b). It is assumed that the stannous octoate react with peroxy radical to produce a cation within the high temperatures of the front. These cations readily react with iodonium salt to continue cationic ring opening of the cycloaliphatic epoxy thereby inhibiting foaming and decarboxylation of the cured resin.

The thermomechanical properties of the two frontally cured resins are given in Table 3. The quality of the specimen obtained with ECC-RICFP was very poor due to large amount of bubbles and foamed patches. Therefore, it was not possible to produce DMA specimens for ECC-RICFP cured specimens.

A large shift in the DSC T_g between first and second heating runs of ECC-RICFP is observed indicating the occurrence of

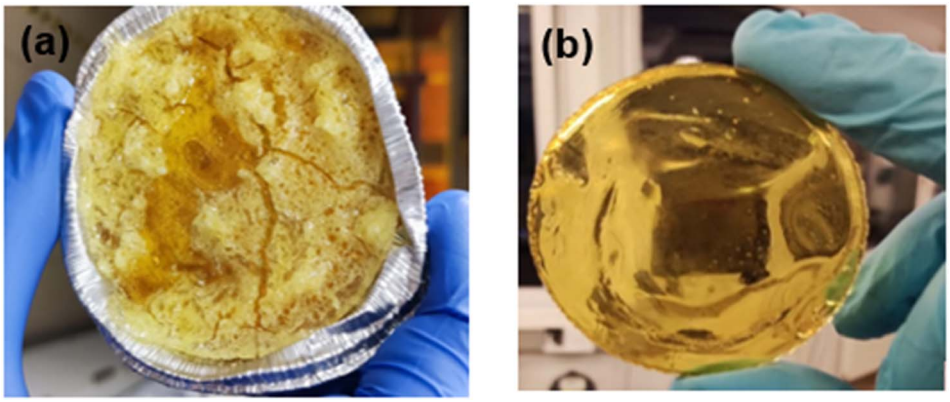

Fig. 9 Photographs of frontally cured (a) ECC-RICFP and (b) ECC-RCFP.

Table 3 Thermomechanical properties of frontally cured cycloaliphatic epoxy resins. Graphs for DMA storage modulus, tan delta and loss modulus are given in ESI

Composition	Mid-point T_g first run (°C)	Mid-point T_g second run (°C)	T_g onset storage modulus (°C)	T_g loss modulus maximum (°C)
ECC-RICFP	61	110	—	—
ECC-RCFP	100	135	100	100

post-curing reactions. ECC-RCFP network gave a higher T_g value than ECC-RICFP. This is related to the ester cleavage of the epoxy monomer, which degrades the network and reduces crosslink density in ECC-RICFP. The T_g from DSC is further verified by DMA experiments (T_g onset storage modulus and maximum of loss modulus). A good correlation further verifies the measured T_g of the ECC-RCFP.

4. Conclusions

This study addressed two pertaining issues in the cationic frontal curing of epoxy monomers namely (i) low degree of curing associated with a medium temperature heat initiation of front and, (ii) decarboxylation during frontal curing of cycloaliphatic epoxies. The results showed positive impact of a stannous octoate/iodonium salt redox couple in increasing the cross-linking density of a medium temperature initiated commercial epoxy resin. The DSC and DMA glass transition temperatures measured for a conventional frontal curing epoxy resin initiated at 150 °C was at 50 °C only, with a large post curing effect. Whereas, the stannous octoate/iodonium salt frontally polymerizable composition not only increased the glass transition temperature of the cured resin by two-fold, but also ensured a high cross-linking density. Uniaxial tensile tests were performed to verify changes in the mechanical strength of the cured resins. The redox frontal cured epoxy resin possessed a higher storage modulus than conventional frontal cured resin, and these thermomechanical properties were equal to the properties of anhydride cured epoxy resin. A quasi-isotropic carbon fiber reinforced composite with a thickness of 20 mm was fabricated and cured with redox frontal curing composition successfully at 150 °C within 30 minutes. The composite was found to be fully intact, almost void free and possessed a high DSC glass transition temperature of 115 °C.

Similar redox composition with cycloaliphatic epoxy initiated with a short UV irradiation dose was found to be fully intact and able to frontally cure. The decarboxylating effect of a peroxide radical during frontal curing of highly reactive cycloaliphatic epoxy was successfully inhibited with the correct amount of stannous octoate in the composition. The results from DSC and DMA measurements confirmed a high glass transition temperature of 100 °C for cycloaliphatic epoxy. These proof-of-concept trials showed that it is possible to control foaming associated with the use of peroxides as radical thermal initiators in the frontal curing of epoxy resins. Furthermore, results from the curing of fiber reinforced composite showed that redox composition would be an alternative rapid route to allow full curing of thick structural composites used in various automobile and aerospace applications.

Conflicts of interest

There are no conflicts to declare.

Acknowledgements

This research work was performed at the Polymer Competence Center Leoben GmbH (PCCL, Austria) under the project "Exploiting frontal polymerization techniques for the efficient and rapid curing of epoxy-based thermosets" (project-no: 1.02). Part of the research work was performed within the COMET-project "Polymers4Hydrogen" (project-no.: 21647053) at the PCCL within the framework of the COMET-program of the Federal Ministry for Climate, Action, Environment, Energy,

Mobility, Innovation and Technology and the Federal Ministry for Digital and Economic Affairs. The PCCL is funded by the Austrian Government and the State Governments of Styria, Lower Austria and Upper Austria.

References

1 J. Staal, E. Smit, B. Caglar and V. Michaud, Thermal management in radical induced cationic frontal polymerisation for optimised processing of fibre reinforced polymers, *Compos. Sci. Technol.*, 2023, **237**, 110009.

2 B. R. Groce, E. E. Lane, D. P. Gary, D. T. Ngo, D. T. Ngo, F. Shaon, J. A. Belgodere and J. A. Pojman, Kinetic and Chemical Effects of Clays and Other Fillers in the Preparation of Epoxy-Vinyl Ether Composites Using Radical-Induced Cationic Frontal Polymerization, *ACS Appl. Mater. Interfaces*, 2023, **15**, 19403–19413.

3 A. D. Tran, T. Koch, P. Knaack and R. Liska, Radical induced cationic frontal polymerization for preparation of epoxy composites, *Composites, Part A*, 2020, **132**, 105855.

4 M. Sangermano, I. Antonazzo, L. Sisca and M. Carello, Photoinduced cationic frontal polymerization of epoxy–carbon fibre composites, *Polym. Int.*, 2019, **68**, 1662–1665.

5 B. A. Suslick, J. Hemmer, B. R. Groce, K. J. Stawiasz, P. H. Geubelle, G. Malucelli, A. Mariani, J. S. Moore, J. A. Pojman and N. R. Sottos, Frontal Polymerizations: From Chemical Perspectives to Macroscopic Properties and Applications, *Chem. Rev.*, 2023, **123**, 3237–3298.

6 F. Hammoud, J. Kirschner, M. Carré, W. Paulus, A.-M. Cristadoro, M. Schmitt and J. Lalevée, Assessment of Photoinduced Frontal Polymerization Processes for a Stable 1K System, *Macromol. Chem. Phys.*, 2023, 1–9.

7 P. Carion, A. Ibrahim, X. Allonas, C. Croutxé-Barghorn and G. L'Hostis, Frontal free-radical photopolymerization of thick samples: applications to LED-induced fiber-reinforced polymers, *J. Polym. Sci., Part A: Polym. Chem.*, 2019, **57**, 898–906.

8 M. S. Malik, S. Schlögl, M. Wolfahrt and M. Sangermano, Review on UV-Induced Cationic Frontal Polymerization of Epoxy Monomers, *Polymers*, 2020, **12**, 1–34.

9 A. D. Tran, T. Koch, R. Liska and P. Knaack, Radical-induced cationic frontal polymerisation for prepreg technology, *Monatsh. Chem.*, 2021, **152**, 151–165.

10 J. A. Pojman, in *Polymer Science: A Comprehensive Reference*, ed. M. Moeller and K. Matyjaszewski, Elsevier BV, Amsterdam, 2012, pp. 957–980.

11 *Epoxy Polymers: New Materials and Innovations*, ed. J. P. Pascault and R. J. J. Williams, John Wiley & Sons, Inc, New York, 2009.

12 J. Masere, Y. Chekanov, J. R. Warren, F. D. Stewart, R. A. Kaysi, J. K. Rasmussen and J. A. Pojman, Gas-free initiators for high-temperature free-radical polymerization, *J. Polym. Sci., Part A: Polym. Chem.*, 2000, **38**, 3984–3990.

13 P. Garra, C. Dietlin, F. Morlet-Savary, F. Dumur, D. Gigmes, J.-P. Fouassier and J. Lalevée, Redox two-component initiated free radical and cationic polymerizations: concepts, reactions and applications, *Prog. Polym. Sci.*, 2019, **94**, 33–56.

14 A. S. Sarac, Redox polymerization, *Prog. Polym. Sci.*, 1999, **24**, 1149–1204.

15 J. W. Breitenbach, A. Springer and K. Horeischy, Die stabilisierende Wirkung des Hydrochinons auf die Wärmepolymerisation des Styrols, *Ber. Dtsch. Chem. Ges. B*, 1938, **71**, 438–441.

16 V. W. Kern, Die katalyse der polymerisation ungesättigter verbindungen mit hilfe von redox systemen, *Makromol. Chem.*, 1948, **1**(3), 209–228.

17 G. V. Schulz, Anregung von Kettenpolymerisationen durch freie Radikale II – Entwicklung der Radikale durch Zersetzung einer Azoverbindung, *Naturwissenschaften*, 1939, **27**, 659–660.

18 D. Wang, P. Garra, J. P. Fouassier and J. Lalevée, Silane/iodonium salt as redox/thermal/photoinitiating systems in radical and cationic polymerizations for laser write and composites, *Polym. Chem.*, 2020, **11**, 857–866.

19 P. Garra, A. Kermagoret, A. Al Mousawi, F. Dumur, D. Gigmes, F. Morlet-Savary, C. Dietlin, J. P. Fouassier and J. Lalevée, New copper(I) complex based initiating systems in redox polymerization and comparison with the amine/benzoyl peroxide reference, *Polym. Chem.*, 2017, **8**, 4088–4097.

20 P. Garra, M. Carré, F. Dumur, F. Morlet-Savary, C. Dietlin, D. Gigmes, J.-P. Fouassier and J. Lalevée, Copper-Based (Photo)redox Initiating Systems as Highly Efficient Systems for Interpenetrating Polymer Network Preparation, *Macromolecules*, 2018, **51**, 679–688.

21 P. Garra, C. Dietlin, F. Morlet-Savary, F. Dumur, D. Gigmes, J.-P. Fouassier and J. Lalevée, Photopolymerization processes of thick films and in shadow areas: a review for the access to composites, *Polym. Chem.*, 2017, **8**, 7088–7101.

22 P. Garra, F. Morlet-Savary, C. Dietlin, J. P. Fouassier and J. Lalevée, On-Demand Visible Light Activated Amine/Benzoyl Peroxide Redox Initiating Systems: A Unique Tool To Overcome the Shadow Areas in Photopolymerization Processes, *Macromolecules*, 2016, **49**, 9371–9381.

23 C. A. Parrinello, C. O. Bounds, M. L. T. Liveri and J. A. Pojman, Thermal frontal polymerization with a thermally released redox catalyst, *J. Polym. Sci., Part A: Polym. Chem.*, 2012, **50**, 2337–2343.

24 H. Yu, Y. Fang, L. Chen and S. Chen, Investigation of redox initiators for free radical frontal polymerization, *Polym. Int.*, 2009, **58**, 851–857.

25 B. McFarland, S. Popwell and J. A. Pojman, Free-Radical Frontal Polymerization with a Microencapsulated Initiator, *Macromolecules*, 2004, **37**, 6670–6672.

26 M. He, X. Huang, Z. Zeng and J. Yang, Photo-triggered redox frontal polymerization: a new tool for synthesizing thermally sensitive materials, *J. Polym. Sci., Part A: Polym. Chem.*, 2013, **51**, 4515–4521.

27 X.-Y. Du, J. Shen, J. Zhang, L. Ling, C.-F. Wang and S. Chen, Generation of a carbon dots/ammonium persulfate redox initiator couple for free radical frontal polymerization, *Polym. Chem.*, 2018, **9**, 420–427.

28 J. V. Crivello and J. H. W. Lam, Redox cationic polymerization: the diaryliodonium salt/ascorbate redox couple, *J. Polym. Sci., Part A: Polym. Chem.*, 1981, **19**, 539–548.
29 A. Formia, J.-M. Tulliani, P. Antonaci and M. Sangermano, Epoxy monomers consolidant for lime plaster cured *via* a redox activated cationic polymerization, *J. Cult. Herit.*, 2014, **15**, 595–601.
30 J. V. Crivello and J. L. Lee, Redox-initiated cationic polymerization: the diaryliodonium salt/benzoin redox couple, *J. Polym. Sci., Polym. Chem. Ed.*, 1983, **21**, 1097–1110.
31 J. V. Crivello and J. L. Lee, Redox initiators for cationic polymerization: the diaryliodonium salt/Sn(II) redox couple, *J. Polym. Sci., Part A: Polym. Chem.*, 1983, **184**, 463–473.
32 J. V. Crivello, Redox initiated cationic polymerization, *J. Polym. Sci., Part A: Polym. Chem.*, 2009, **47**, 1825–1835.
33 J. V. Crivello, Redox initiated cationic polymerization: the unique behavior of alkyl glycidyl ethers, *J. Polym. Sci., Part A: Polym. Chem.*, 2011, **49**, 2147–2154.
34 J. V. Crivello, Redox initiated cationic polymerization: reduction of diaryliodonium salts by 9-BBN, *J. Polym. Sci., Part A: Polym. Chem.*, 2009, **47**, 5639–5651.
35 J. V. Crivello, *US Pat.*, 4216288, 1980.
36 D. Bomze, P. Knaack and R. Liska, Successful radical induced cationic frontal polymerization of epoxy-based monomers by C–C labile compounds, *Polym. Chem.*, 2015, **6**, 8161–8167.
37 R. Liska, D. Bomze, W. Kern and P. Knaack, *US Pat.*, 10738146B2, 2020.
38 J. A. Pojman, Traveling fronts of methacrylic acid polymerization, *J. Am. Chem. Soc.*, 1991, **113**, 6284–6286.
39 W. Jakubowski, K. Min and K. Matyjaszewski, Activators Regenerated by Electron Transfer for Atom Transfer Radical Polymerization of Styrene, *Macromolecules*, 2006, **39**, 39–45.
40 N. V. Tsarevsky and K. Matyjaszewski, "Green" atom transfer radical polymerization: from process design to preparation of well-defined environmentally friendly polymeric materials, *Chem. Rev.*, 2007, **107**, 2270–2299.
41 F. Yilmaz, A. Sudo and T. Endo, Allyl sulfonium salt as a novel initiator for active cationic polymerization of epoxide by shooting with radicals species, *J. Polym. Sci., Part A: Polym. Chem.*, 2010, **48**, 4178–4183.
42 X. Fernàndez-Francos, S. G. Kazarian, X. Ramis and À. Serra, Simultaneous monitoring of curing shrinkage and degree of cure of thermosets by attenuated total reflection Fourier transform infrared (ATR FT-IR) spectroscopy, *Appl. Spectrosc.*, 2013, **67**, 1427–1436.
43 International Organization for Standardization (ISO), *DIN EN ISO 11357 Plastics – Differential Scanning Calorimetry (DSC). Part 1: General Principles*, 2016.
44 International Organization for Standardization (ISO), *DIN EN ISO 6721-5 Plastics – Determination of Dynamic Mechanical Properties. Part 5: Flexural Vibration – Non-resonance Method*, **https://www.iso.org/standard/73145.html**, accessed 20 April 2022.
45 International Organization for Standardization (ISO), *DIN EN ISO 527-2 Determination of Tensile Properties. Part 2: Test Conditions for Moulding and Extrusion Plastics*, 1996.
46 Y. Ma, Z. Liu, X. Qian, Y. Zhao, M. Li and P. Li, Effect of Excessive Iodonium Salts on the Properties of Radical-Induced Cationic Frontal Polymerization (RICFP) of Epoxy Resin, *Ind. Eng. Chem. Res.*, 2023, **62**, 4896–4904.
47 M. S. Malik, M. Wolfahrt, M. Sangermano and S. Schlögl, Effect of a Dicycloaliphatic Epoxide on the Thermo-Mechanical Properties of Alkyl, Aryl Epoxide Monomers Cured *via* UV-Induced Cationic Frontal Polymerization, *Macromol. Mater. Eng.*, 2022, **307**, 1–10.
48 G. W. Ehrenstein, *Thermal Analysis of Plastics: Theory and Practice*, Hanser, Munich, 2004.
49 R. Schwalm, UV-härtende Automobildecklacke rücken näher: Einfluss der Vernetzung UV-härtbarer Beschichtungen auf Kratzfestigkeit, Härte und Flexibilität, *Farbe Lack*, 2000, **106**, 58–69.
50 P. Bajaj, N. K. Jha and R. A. Kumar, Effect of coupling agents on the mechanical properties of mica/epoxy and glass fiber/mica/epoxy composites, *J. Appl. Polym. Sci.*, 1992, **44**, 1921–1930.
51 J. P. Greene, *Automotive Plastics and Composites: Materials and Processing*, William Andrew Applied Science Publishers, 2021.
52 D. P. Gary, S. Bynum, B. D. Thompson, B. R. Groce, A. Sagona, I. M. Hoffman, C. Morejon-Garcia, C. Weber and J. A. Pojman, Thermal transport and chemical effects of fillers on free-radical frontal polymerization, *J. Polym. Sci.*, 2020, **58**(16), 2267–2277.
53 U. Bulut and J. V. Crivello, Investigation of the Reactivity of Epoxide Monomers in Photoinitiated Cationic Polymerization, *Macromolecules*, 2005, **38**, 3584–3595.